

Received 21 April 2022, accepted 6 June 2022, date of publication 15 July 2022, date of current version 1 August 2022.

Digital Object Identifier 10.1109/ACCESS.2022.3191349

A New Current Transducer for On-Line Monitoring of Leakage Current on HV Insulator Strings

RODRIGO J. VILLALOBOS^{1,2}, LUIS A. MORAN², (Fellow, IEEE), FERNANDO HUENUPÁN¹, FRANCISCO VALLEJOS¹, ROBERTO MONCADA¹, AND CRISTIAN PESCE G.¹, (Member, IEEE)

¹Department of Electrical Engineering, Universidad de La Frontera, Temuco 4811230, Chile

²Department of Electrical Engineering, Universidad de Concepción, Concepción 4030000, Chile

Corresponding author: Rodrigo J. Villalobos (rodrigo.villalobos@ufrontera.cl)

This work was supported in part by the Conicyt Fondef/Cuarto Concurso IDeA en Dos Etapas del Fondo de Fomento al Desarrollo Científico y Tecnológico, Fondef/Conicyt 2017, under Grant ID17I20421; and in part by the Dirección de Investigación, Universidad de La Frontera.

ABSTRACT Leakage current measurement and its harmonics have been widely used for the pollution level estimation of HV insulator strings. However, the solutions available to applications into transmission lines and substations are few and it reduces the creepage distance (mm/kV), must be installed by de-energizing the electrical power system or do not allow the characteristic harmonics of the leakage current to be obtained. This paper presents the design, implementation, testing, and experimental validation of a transducer for measuring and online monitoring of leakage currents on high-voltage insulator strings. The transducer is composed of a clamp-type current transformer with a supermalloy material core. The leakage current is reconstructed from the transducer output voltage by applying the Fast Fourier Transform (FFT) and its own inverse transfer function, which allows it to obtain the leakage current with its characteristic harmonics and reduces the electromagnetic noise present in power systems. The output voltage of the transducer was acquired, processed, and transmitted using a dedicated device installed in the HV tower. The proposed transducer was first tested on an insulator inside an artificial fog chamber according to the IEC 60507 standard. The transducer was experimentally validated on an insulator string in a 220 kV substation. The results showed that the designed transducer measured the leakage current and its harmonics with an average error less than 1.76%. With these results the transducer can be used for the on-line monitoring of pollution levels of insulator strings without reduces the creepage distance.


INDEX TERMS Current transducer, HV insulator strings, leakage current, on-line monitoring, pollution level estimation.

I. INTRODUCTION

Insulator strings in overhead transmission lines present one of the highest failure rates in electric power transmission systems [1]. Their exposure to different environmental pollutants combined with climatic factors and humidity decreases the insulation capacity of the insulator string [2], which is manifested by an increase in the amplitude and distortion of the leakage current that circulates on the surface of the

insulator [3]. A considerable increase in the leakage current may cause a ground failure called a flashover [4]. In many cases, this failure causes circuit breakers to open in substations adjacent to the power lines, generating significant economic losses for the transmission companies and harming the development of industrial activity and the quality of life of the people [5].

Pollutants based on dust, soluble salts, or chemical emissions are deposited on the surface of insulators, promoting the generation of dry bands that modify the waveform of the leakage current [3]–[6]. The characteristic harmonics found

The associate editor coordinating the review of this manuscript and approving it for publication was Ahmed F. Zobaa .

in these currents are odd, and are mainly found between the first and eleventh harmonics [7], [8].

Numerous authors have presented different techniques to obtain the pollution level of insulators from the analysis of some parameters of the leakage current [9], [10]. Therefore, the leakage current may be considered one of the most important pollution level indicators in the literature [11], [12], [13].

Some parameters calculated from the measurement of the leakage current are as follows: the root-mean-square (RMS) value, maximum amplitude, number of pulses, harmonic spectrum, total harmonic distortion (THD), change in amplitude of some harmonics (3rd, 5th and 7th) and the association between them. These have been described and are directly related to the different degrees or levels of pollution on insulators [14]–[17].

The classification of pollution levels is presented by the IEC 60815 standard [18] and is directly related to the amount of pollutant adhered to the insulator surface, established by the ESDD (Equivalent Salt Deposit Density) and the NSDD (Non-Soluble Surface Deposits) [19]. It should be noted that previous studies have defined associations between the increase in some parameters of the leakage current and the increase in ESDD [3].

However, electrical utility companies are required to estimate the pollution level of insulator strings in real time to efficiently plan the maintenance of their power lines by washing them with distilled water under pressure [20]. The washing programs are specific to each company and are determined based on different mechanisms, such as experience, laboratory conductivity measurement of the contamination deposited on the control insulator part of test stations, and leakage current measurement equipment that works mainly connected in series to the insulator strings. This solution can affect the insulation capacity of an insulator string. Among the solutions available for real-time monitoring, those presented in [21] are worth noting because they develop a satellite network for the remote monitoring of lines of 220 and 500 kV, or by [5], who developed a remote unit with a GPRS connection. Both solutions measure the leakage current using an optical sensor connected in series to the string.

In recent years, there has been an important development in the way the pollution level is determined according to the leakage current; however, solutions to measure the leakage current on the insulator strings of transmission lines and substations without affecting the insulation are limited.

Some prominent methods for measuring the leakage current are the aforementioned fiber-optic sensors, which are connected in series to obtain an optical signal with modulated amplitude. This method makes it possible to obtain a full waveform and is highly immune to magnetic noise. In addition, other authors [10]–[22] used a collector ring consisting of a metal ring attached to the insulator cap that bypassed the current. This system allows the current signal to be obtained by passing the current through a shunt resistance, which determines the current by measuring the voltage drop across the resistor. These alternatives are based on diverting the

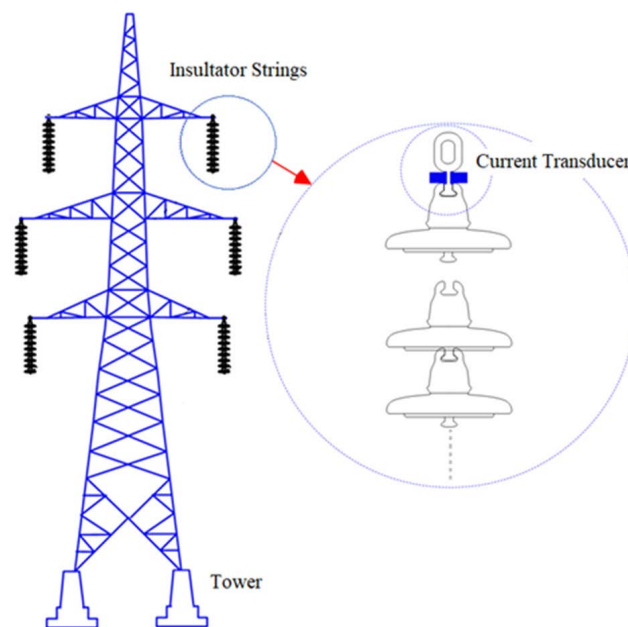


FIGURE 1. Current transducer on insulator string.

leakage current between the last and penultimate insulators of the string, connecting different sensors in parallel, which could decrease the creepage distance (mm/kV) because the last insulator is bypassed.

Another author presented a condition-monitoring insulator based on the output voltage and its harmonics with a Rogowski coil transducer [23]. This technique determines the pollution level without reconstructing the leakage current. Therefore, its use is limited to its own technique for obtaining the pollution level in the output voltage.

Finally, a method to determine the pollution level based on the leakage current has been used in numerous articles in recent years. However, the solutions proposed for measuring this current are invasive and deviate from the current on the last insulator closest to the metallic structure. This paper presents a new proposal to measure the leakage current that can be used for online monitoring and permanently on insulator strings. The insulation capacity was not affected, and the installation procedure could be performed without affecting the operation of the power system.

The design, implementation, and evaluation of the non-invasive current transducer with a toroidal core made of supermalloy material with high permeability to obtain a greater amplitude of output voltage are presented (Fig. 1). The output of the current transformer was amplified using an electronic circuit attached to it. The transducer housing was airtight, made of aluminum, and connected to the ground of the power system. This transducer has been tested in the laboratory for different frequencies and leakage current amplitudes, as well as in a 220 kV substation. Through this set of tests, it was confirmed that the transducer meets the required performance and can be used to obtain the pollution

TABLE 1. Core characteristics.

Description	Value
Internal radius (R_i)	1.6×10^{-2} m
External radius (R_o)	2.1×10^{-2} m
Core height (h)	5.0×10^{-2} m
Core width (d)	5.0×10^{-2} m
Secondary Turn (N_s)	8000
Air gap (l_g)	1.0×10^{-5} m
Core material	Supermalloy

level based on the measurement of the leakage current, and has been used in the field for online monitoring.

II. CURRENT TRANSDUCER DESIGN

The transducer was designed for use on insulator strings, extensively using a cap and pin type insulator. This characteristic imposes a limitation on the physical design because the transducer must have sufficient dimensions to be installed on the fitting that holds the insulator with a metallic structure (tower). Other limitations do not affect the insulation capacity of the string, being immune to noise, and measuring very low-amplitude currents (μA and mA). Thus, it must also have a sufficient bandwidth to measure the 7th or 11th harmonic, according to the needs presented by different authors [24]–[27] in the analysis of the leakage current.

The current transducer is composed of a transformer with a magnetic core and an electronic circuit designed to amplify the output signal of the transducer. The output voltage is connected to a shielded conductor, which is designed to provide measurements to a dedicated data acquisition, processing, and transmission device located in the lower part of the HV tower. This device is responsible for sending data wirelessly to a control center, where they are processed using the technique described below.

Both the electronic circuit of the transducer and the data acquisition, processing, and transmission devices are supplied from an independent energy source made up of a 100 W photovoltaic module, lithium batteries (storage system), and a voltage regulator that provides 12V and 5V.

A. CHOICE OF CORE GEOMETRY, MATERIALITY AND ISOLATION

The core is designed to be installed in a non-invasive manner to fit the last insulator of the string, which is connected to the metallic structure, as shown in Fig. 1. The core was chosen to have a toroidal shape with two air gaps (clamp type). The primary corresponds to the pin or fitting of the insulator, and the secondary corresponds to a winding with 8,000 turns. The primary technical characteristics are listed in Table 1.

The high permeability of the Supermalloy core offers high magnetic permeability and low reluctance, which favors the measurement of low currents. For low currents it is convenient to use materials that require a low field strength for magnetization [28]. The Supermalloy material corresponds to an alloy of nickel (79%), iron (17%) and molybdenum (4%),

TABLE 2. Parameters used in the design.

DESCRIPTION	Symbol
Vacuum permeability	μ_0
Relative permeability of the material	μ_r
Air gap length	l_g
Core cross section thickness	d
Internal radius	R_i
External radius	R_o
Frequency	f

with which a higher output voltage amplitude can be obtained for low input currents compared to a pure iron or ferrite core [29].

The transducer was designed to be installed exclusively in the insulator fitting connected to the HV tower (on the first insulator); therefore, it was exposed to a potential of 0 V. In any case, the transducer fulfills the requirements of protection against partial discharges (PD) should some particular faults occur in the electrical power system.

The transformer core was insulated from the secondary windings with NOMEX paper of high inherent dielectric strength (30-40 mm/kV). The insulator fitting is insulated from the metallic transducer using a silicone cylinder that also generates a significant clearance distance of 106 mm and creepage distance of 135 mm, fulfilling the recommendation of the IEC 60644-1 standard for 100 kV (maximum value). In addition, the housing is grounded with a conductor that screens and protects the active part of the transducer from the electrical fields that could interfere with the correct measurement of the leakage current, offering a low-impedance path in case of an important potential difference.

B. TRANSDUCER GAIN

The gain of the transducer is calculated as a combination of the gain of the transformer and the gain of the electronic amplification circuit. For the transformer, the gain is defined as the ratio between the output voltage (V_s) and the primary current (I_m), as given in Equation 1. Where V_s is calculated as the proportion of the number of turns (N_s) to the derivative of the magnetic flux (ϕ) in the core.

$$V_s = N_s \frac{d}{dt}(\phi) \quad (1)$$

Considering that the magnetic flux depends on the reluctance and coil current, the gain expression expressed in Equation 2 was deduced.

$$G_{tr} = \frac{V_s}{I_m} = \frac{2\pi f N_s \mu_0 \mu_r (R_o - R_i)^2}{\pi (R_o + R_i) + 2l_g \mu_r} \quad (2)$$

Equation (2) shows that the gain of the transformer is independent of the amplitude of the input current but linearly dependent on the frequency of the same current. Table 2 lists the nomenclature for the variables used in the design.

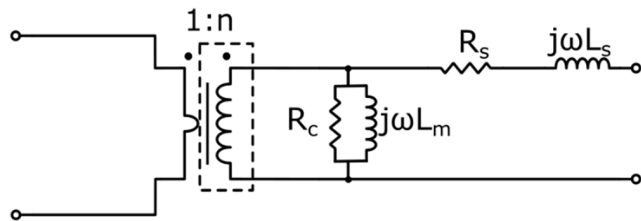


FIGURE 2. Transformer parameters.

The electronic circuit was designed with an operational amplifier type INA121P, which is part of the transducer and is attached to the transformer. The circuit was fed from a power source provided by the acquisition and measurement data processing device located at the bottom of the HV tower. The gain of the electronic circuit is shown in (3), the value of which is given by the input resistance, R_G . The value of this resistance was 50 k Ω to obtain a maximum voltage transducer limited by the maximum input voltage of the acquisition, processing, and transmission data device.

However, the maximum output voltage must be associated with the maximum current expected on the insulator, which was set to 300 mA.

The amplification circuit has a constant gain throughout the operating range (50–550 Hz), as defined in Equation 3.

$$G_{AO} = 1 + \frac{50k}{R_G} \quad (3)$$

Finally, the transducer gain (G_{Tr}) is defined as a combination of Equations 2 and 3, and is defined as shown in Equation 4.

$$G_{Tr} = \frac{V_{STr}}{I_m} = 4\pi \cdot f \cdot A_{tr} \quad (4)$$

where V_{STr} is the output voltage of the transducer and A_{tr} is a constant that depends on the physical and magnetic design parameters of the current transformer and the gain of the amplification circuit. Equation 4 shows the gain of the transducer, which is directly proportional to the frequency of the primary current.

C. TRANSDUCER PARAMETERS

Using DC resistance measurements and short-circuit and open-circuit tests, the parameters of the simplified transformer model were obtained, as shown in Fig. 2. The primary resistance (R_p) and leakage inductance of the primary (L_{pk}), can be disregarded because of the characteristics of the primary. Table 3 lists the values obtained for the secondary resistance (R_s), leakage inductance of the secondary (L_{sk}), magnetizing inductance (L_m) and the loss resistance in the core (R_c).

The large number of turns in the core (8000 units) produces a high leakage inductance in the secondary, even when carefully and homogeneously wrapping the enameled conductor around the core. However, this inductance and resistance do not produce a relevant voltage drop in the secondary circuit, and they do not affect the voltage regulation owing to the

TABLE 3. Transformer parameters.

DESCRIPTION	Value
R_s	416 Ω
L_{sk}	11.3 H
L_m	123 H
R_c	275 Ω

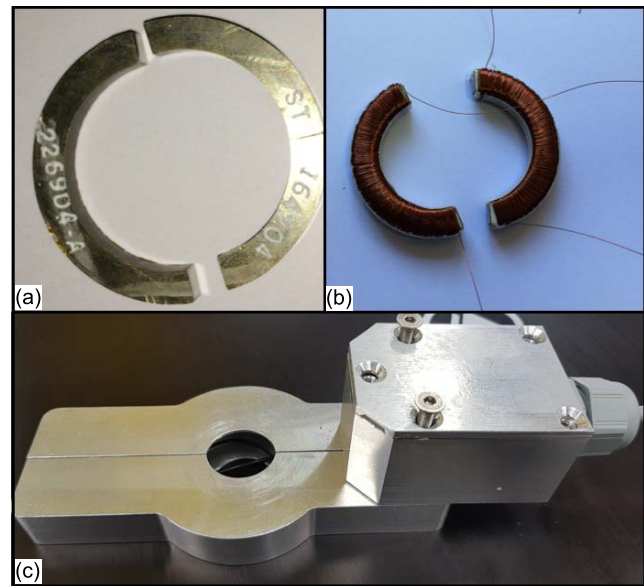


FIGURE 3. Current transducer construction process. (a) Supermalloy core. (b) Core with secondary coil with copper cable of 0.2 mm diameter. (c) Aluminum housing of the transformer and circuit amplifier.

high impedance differential ($1 \cdot 10^{12} \Omega$) of the amplifier circuit (INA121P) connected to the transformer output.

On the other hand, the transformer parasitic input-output capacitance were measured and its value was of 17 pF. This value does not allow important common-mode current circulation because the harmonic characteristics are mainly between 50 and 550 Hz and not at high frequencies, as in other applications [30].

III. CONSTRUCTION AND EVALUATION

The transducer manufacturing process for measuring the leakage in high-voltage insulator strings is described. The construction is based on the design presented in Section II. The evaluation of the prototype at a low voltage is detailed, and the experimental gain is shown. The results of the tests performed on the transducer at medium and high voltages are highlighted.

A. CONSTRUCTION

This section presents the results of the transducer construction based on the design described. Fig. 3 (a) and 3 (b) show the supermalloy core and the 0.2 mm enameled copper wound core with 4000 turns on each half toroid, respectively. Fig. 3 (c) shows the current transducer and electronic circuit

TABLE 4. Physical design.

DESCRIPTION	mm
Length	133
Width	42
Height	16
Internal radius	10.8
External radius	30
Length (Amplifier Circuit box)	60
Width (Amplifier Circuit box)	42
Height (Amplifier Circuit box)	30

encapsulated in an aluminum housing. The package was grounded in an electrical system to dissipate electromagnetic noise.

The physical dimensions of the transducer housing are shown in Table 4.

B. EXPERIMENTAL ESTIMATION OF GAIN AND PHASE SHIFT

On insulator strings used at 220 kV, the leakage current presents amplitudes ranging from microamperes to milliamperes [11].

To determine the gain and phase of the transducer in terms of frequency, experimental tests were carried out for each of the characteristic harmonics of the leakage current, up to the 11th harmonic, and with different values of current amplitude for each of the harmonics. The frequency response of the transducer was obtained for different amplitudes and frequencies.

The transducer gain is defined as the association between the peak voltage value of the output transducer (V_{peak}) and the peak current value of the primary (I_{peak}) for each frequency of the characteristic harmonic $\omega_h(2\pi f_h)$ as given in Equation 5.

$$G(\omega_h) = \frac{V_{peak}}{I_{peak}} \tag{5}$$

The phase shift was calculated as the difference between the angle of the output voltage (φ_{output}) and the angle of the primary current (φ_{input}), as shown in Equation 6.

$$\theta(\omega_h) = \varphi_{output} - \varphi_{input} \tag{6}$$

The results of the tests carried out for different current amplitudes and frequencies are shown in Fig. 4 (a). Here, it can be observed that the gain has a linear performance and is directly related to the frequency of the primary current. Furthermore, the gain of the transducer was independent of the current amplitude. Fig. 4 (b) shows the phase of the transducer in terms of frequency. Notably, the phase shift is close to 90°, with a slight dependence on the frequency. Knowing the performance of the transducer as a function of frequency in terms of gain and phase, it is possible to determine its transfer function.

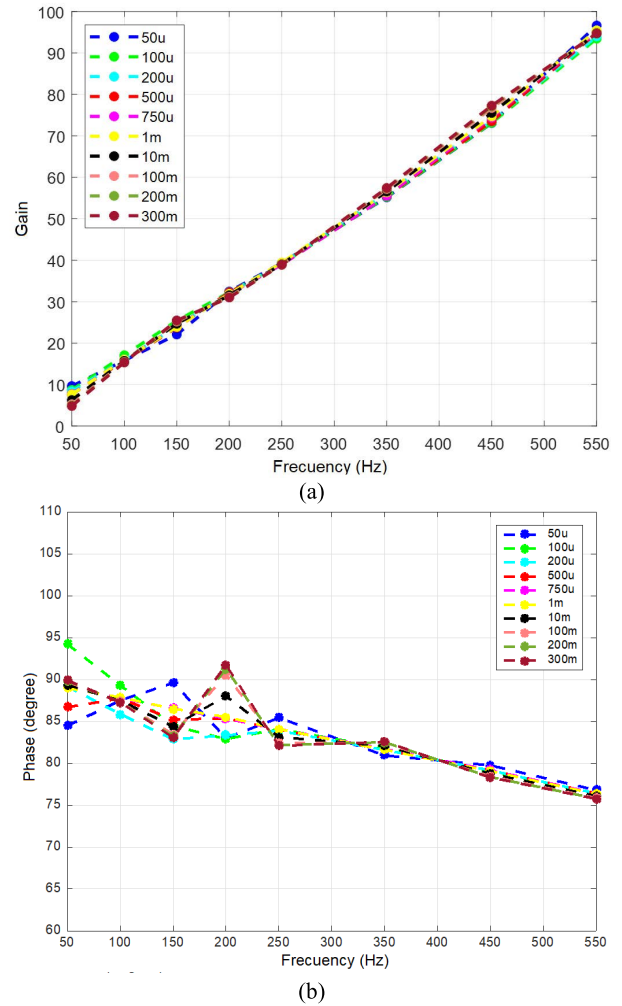


FIGURE 4. Transducer frequency response. (a) Gain. (b) Phase.

To obtain the leakage current measured in the insulator from the output voltage of the transducer, and the gain of the transducer, the fast Fourier transform (FFT) is used. The FFT up to the 11th harmonic was calculated from the output voltage of the transducer, and an inverse transfer function was applied. Therefore, the reconstructed leakage current is obtained. It should be noted that the use of the FFT also allows the signal to be filtered by eliminating non-characteristic harmonics from the output voltage, and therefore, also from the reconstituted leakage current.

From these experimental results, it can be concluded that the current transducer can measure currents ranging from 50 μA to at least 300 mA. This wide measurement range allows the use of any technique for pollution level determination based on leakage current for all types of insulators and creepage distances present in power systems. This characteristic differs from others, which shows results for ranges from 5 to 60 mA and that necessarily decrease the creepage distance of the string. In addition, this solution differs from other solutions that could have a similar measurement range,



FIGURE 5. Experimental implementation in the laboratory.

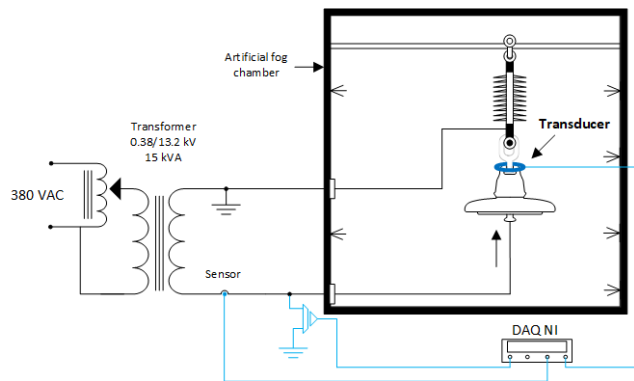


FIGURE 6. Medium voltage leakage current measurement set-up.

but it must be installed to de-energize the power system where it is connected.

C. MEDIUM VOLTAGE TRANSDUCER TESTS

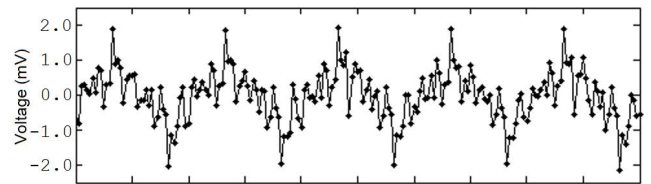
An artificial fog chamber based on the IEC 60507 standard [31] was constructed to obtain measurements of the leakage current on the cap- and pin-type insulators.

Fig. 5 shows the leakage current transducer on the insulator inside the artificial fog chamber.

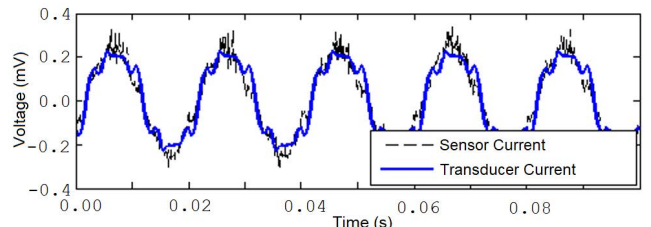
Fig. 6 shows the setup of the test, where the insulator and transducer are subjected to a voltage of 9 kV, which is regulated through a 380 V single-phase Variac. The current that circulates through the insulator is measured using a transducer and commercial current sensor. Data were acquired and processed by a National Instrument acquisition and processing card and displayed using LabView software. For these tests, the sprinklers in the artificial fog chamber were controlled to internally generate a relative humidity of 95%.

Fig. 7(a) shows the output voltage of the transducer, which was measured using a voltage probe connected to the National Instruments device. Fig. 7(b) presents the results of the leakage current on the insulator, one obtained by a standard micrometer and the other by the transducer.

In Fig. 8(a) and 8(b), the harmonic spectra for these currents are presented. It can be observed that the constructed leakage current has characteristic harmonics of the leakage current in this type of insulator.

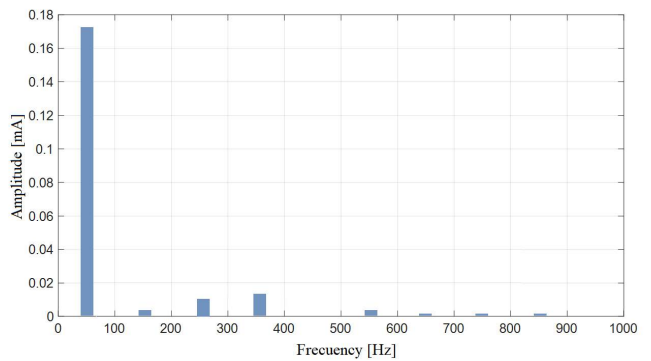


(a)

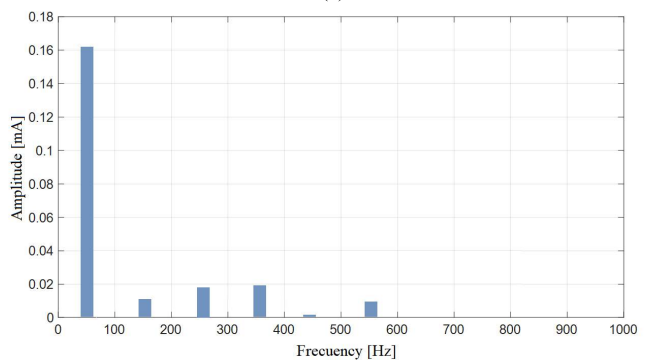


(b)

FIGURE 7. Insulator testing waveforms. (a) Transducer output voltage; (b) Standard microammeter (black) and transducer current (blue).



(a)



(b)

FIGURE 8. Frequency spectrum for the measured current. (a) Standard microammeter. (b) Transducer current.

Likewise, it has similar amplitudes to those measured by the other sensor.

It is noted that At 50 Hz, the amplitude of the current measured by the commercial micrometer was 0.168 mA, and that one measured by the transducer was 0.160 mA, with a difference of 3.9%. A similar occurs with the 3rd, 5th, 7th, 9th, and 11th harmonics, where the average difference is 1.23%. These results indicate that the transducer functions correctly

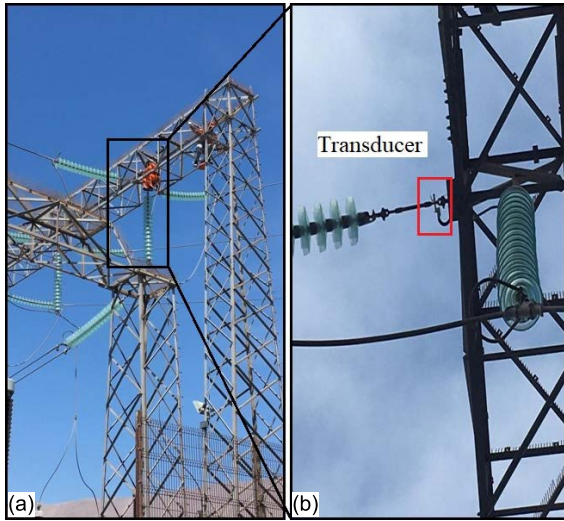


FIGURE 9. On-site installation at the Tarapacá substation. (a) Insulator string and line frame (Left). (b) Current transducer (Right).

when installed on the insulator fitting and is subjected to a nominal voltage for the insulator (9 kV).

This section shows a known frequency response for the current transducer up to the 11th harmonic, which allows it to be used for pollution-level estimation based on the harmonics of the leakage current.

The developments presented in the literature, such as those already mentioned [21], show some measurements in RMS values until 60 mA, and its harmonics are not known.

D. TESTING IN A 220 kV SUBSTATION

The 220 kV Tarapacá substation is located in the desert of northern Chile, 100 m from the Pacific Ocean, and presents important industrial activity around it, which allows the transducer to be tested in a saline and highly contaminated environment. For a full-scale evaluation, the transducer was installed in one of the energized insulator strings of this substation. Its installation was performed in the insulator fitting closest to the metal structure, and its output was connected to a shielded conductor in charge of transmitting the data to the data acquisition and processing device located in the lower part of the HV tower.

This device has been specially designed for the transducer and is capable of wirelessly acquiring and transmitting transducer data through LoRa technology to a control center. These data are uploaded to the Internet and processed on a PC with access to the Internet. This process involves calculating the FFT of the signal measured by the transducer and applying the inverse transfer function obtained previously.

Fig. 9 (a) shows a photograph of the insulator string, where the transducer was installed by specialized personnel at a height of 20 m in a metallic structure line frame. In Fig. 9 (b), the transducer already installed in the insulator fitting, specifically in the tensioner of the insulator closest to the metallic structure, is observed. The cable responsible for

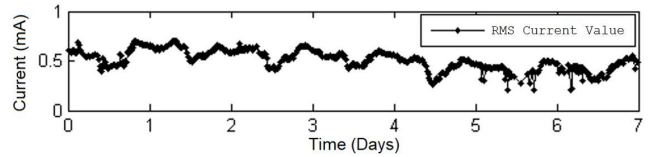


FIGURE 10. RMS current value in the Tarapacá substation.

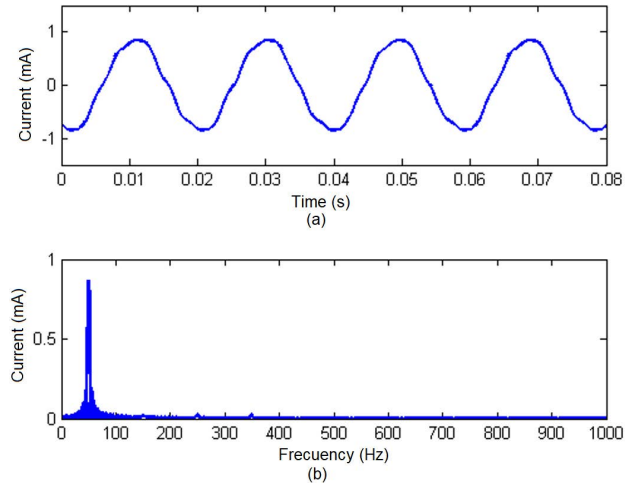


FIGURE 11. Measurements in the Tarapacá substation. (a) Current waveform. (b) Harmonic spectrum of the current.

transporting data from the transducer to the acquisition device is also illustrated. The data measured by the transducer and transmitted by the acquisition device were processed in a PC several hundreds of kilometers from the Tarapacá substation.

In this article, the data obtained from the leakage current measurement over a period of one week are shown. The leakage current reconstructed using the proposed technique is shown in Fig. 10. The figure shows that the leakage current has an average value of 0.48 mA that fluctuates between 0.22 and 0.65 mA. This fluctuation has a 24-hour periodicity and depends on the humidity, which for the area is associated with day and night. Specifically, the leakage current increases in amplitude during the early morning hours when humidity increases.

Fig. 11 (a) shows the waveform of the current reconstructed for an instant when the humidity is high (90%) but with low pollution on the insulator. Fig. 11(b) shows the harmonic spectrum of this current with harmonics of the 3rd, 5th, and 7th orders with amplitude values below 3%. Similar values of leakage current harmonics can be found in the article [8], where the 3rd and 5th harmonics reach values between 2.5 and 3% for a purely sinusoidal applied voltage or with low harmonics. The calculated THD reached a value of 14.8% under the conditions described above.

IV. CONCLUSION

A new transducer designed and manufactured to measure the leakage currents on HV insulator strings is presented.

The gain and phase shift of the transducer for the relation between the output voltage and the primary current of the

transducer was experimentally calculated until the 11th harmonic. The obtained gain increases linearly with frequency, and the phase shift is known to be close to 90° . These characteristics allow the leakage current to be reconstructed as a function of the measured output voltage, filtering out unwanted harmonics, such as those produced by the electromagnetic noise of power systems.

The design of a current transducer with a core made of supermalloyed material with high magnetic permeability, together with a winding of 8000 turns on the secondary, allows the generation of a voltage of at least 2 mV amplitude on the secondary side of the transformer, which can be acquired to measure and calculate the leakage current in the insulator string, as has been shown in laboratory and field tests.

The current amplitude and waveform measured by the current transducer were compared with those of a commercial leakage current sensor (in an artificial fog chamber). The results showed a difference of 3.90% in the first harmonic and less than 1.23% in the higher harmonics. These differences can be neglected for the measurement of the leakage current on insulators because high precision is not required for the fundamental current value.

The transducer was installed on an insulator string without interrupting the operation of the power system or affecting the insulation capacity (mm/kV) of the insulator string. The measured current was of 0.42 mA comparable to the 0.2 mA obtained in the artificial fog chamber and to the 0.4 mA in other articles at 220 kV.

The results indicate that the transducer makes it possible to accurately measure the leakage current present on insulator strings, which constitutes a very effective tool for determining the pollution level. This can be an important support for defining cleaning programs aimed at reducing failure rates and increasing the continuity of service of transmission lines and electrical substations.

REFERENCES

- [1] *Polluted Insulators: A Review of Current Knowledge*, CIGRÉ Working Group, Paris, France, Jun. 2000.
- [2] J. Y. Li, C. X. Sun, W. X. Sima, and Q. Yang, "Stage pre-warning based on leakage current characteristics before contamination flashover of porcelain and glass insulators," *IET Gener., Transmiss. Distrib.*, vol. 3, no. 7, pp. 605–615, Jul. 2009, doi: [10.1049/iet-gtd.2008.0604](https://doi.org/10.1049/iet-gtd.2008.0604).
- [3] J. Li, W. Sima, C. Sun, and S. A. Sebo, "Use of leakage currents of insulators to determine the stage characteristics of the flashover process and contamination level prediction," *IEEE Trans. Dielectr. Electr. Insul.*, vol. 17, no. 2, pp. 490–501, Apr. 2010, doi: [10.1109/TDEI.2010.5448105](https://doi.org/10.1109/TDEI.2010.5448105).
- [4] S. Zhao, X. Jiang, Z. Zhang, J. Hu, and L. Shu, "Flashover voltage prediction of composite insulators based on the characteristics of leakage current," *IEEE Trans. Power Del.*, vol. 28, no. 3, pp. 1699–1708, Jul. 2013, doi: [10.1109/TPWRD.2013.2257879](https://doi.org/10.1109/TPWRD.2013.2257879).
- [5] M. M. Werneck, D. M. dos Santos, C. C. de Carvalho, F. V. B. de Nazaré, and R. C. da Silva Barros Allil, "Detection and monitoring of leakage currents in power transmission insulators," *IEEE Sensors J.*, vol. 15, no. 3, pp. 1338–1346, Mar. 2015.
- [6] L. Lan, G. Zhang, Y. Wang, X. Wen, W. Wang, and H. Pei, "The influence of natural contamination on pollution flashover voltage waveform of porcelain insulators in heavily polluted area," *IEEE Access*, vol. 7, pp. 121395–121406, 2019, doi: [10.1109/ACCESS.2019.2936868](https://doi.org/10.1109/ACCESS.2019.2936868).
- [7] D. Maadjoudj, A. Mekhaldi, and M. Tegar, "Flashover process and leakage current characteristics of insulator model under desert pollution," *IEEE Trans. Dielectr. Electr. Insul.*, vol. 25, no. 6, pp. 2296–2304, Dec. 2018, doi: [10.1109/TDEI.2018.007112](https://doi.org/10.1109/TDEI.2018.007112).
- [8] R. Ghosh, B. Chatterjee, and S. Chakravorti, "A novel leakage current index for the field monitoring of overhead insulators under harmonic voltage," *IEEE Trans. Ind. Electron.*, vol. 65, no. 2, pp. 1568–1576, Feb. 2018, doi: [10.1109/TIE.2017.2733490](https://doi.org/10.1109/TIE.2017.2733490).
- [9] S. Deb, S. Das, A. K. Pradhan, A. Banik, B. Chatterjee, and S. Dalai, "Estimation of contamination level of overhead insulators based on surface leakage current employing detrended fluctuation analysis," *IEEE Trans. Ind. Electron.*, vol. 67, no. 7, pp. 5729–5736, Jul. 2020, doi: [10.1109/TIE.2019.2934008](https://doi.org/10.1109/TIE.2019.2934008).
- [10] J. Wang, Y. Xi, C. Fang, L. Cai, J. Wang, and Y. Fan, "Leakage current response mechanism of insulator string with ambient humidity on days without rain," *IEEE Access*, vol. 7, pp. 55229–55236, 2019, doi: [10.1109/ACCESS.2019.2910660](https://doi.org/10.1109/ACCESS.2019.2910660).
- [11] H. de Santos and M. A. S. Bobi, "A cumulative pollution index for the estimation of the leakage current on insulator strings," *IEEE Trans. Power Del.*, vol. 35, no. 5, pp. 2438–2446, Oct. 2020, doi: [10.1109/TPWRD.2020.2968556](https://doi.org/10.1109/TPWRD.2020.2968556).
- [12] W. Chen, C. Yao, P. Chen, C. Sun, L. Du, and R. Liao, "A new broadband microcurrent transducer for insulator leakage current monitoring system," *IEEE Trans. Power Del.*, vol. 23, no. 1, pp. 355–360, Jan. 2008, doi: [10.1109/TPWRD.2007.905833](https://doi.org/10.1109/TPWRD.2007.905833).
- [13] M. Khalifa, A. El-Morshehy, O. E. Gouda, and S. E. D. Habib, "A new monitor for pollution on power line insulators. Part 2: Simulated field tests," *IEE Proc. C, Gener., Transmiss. Distrib.*, vol. 135, no. 1, pp. 24–30, 1988, doi: [10.1049/ip-c.1988.0003](https://doi.org/10.1049/ip-c.1988.0003).
- [14] A. A. Salem, R. Abd-Rahman, S. Ahmed Al-Gailani, M. S. Kamarudin, H. Ahmad, and Z. Salam, "The leakage current components as a diagnostic tool to estimate contamination level on high voltage insulators," *IEEE Access*, vol. 8, pp. 92514–92528, 2020, doi: [10.1109/ACCESS.2020.2993630](https://doi.org/10.1109/ACCESS.2020.2993630).
- [15] J. Li, C. Sun, W. Sima, Q. Yang, and J. L. Hu, "Contamination level prediction of insulators based on the characteristics of leakage current," *IEEE Trans. Power Del.*, vol. 25, no. 1, pp. 417–424, Jan. 2010, doi: [10.1109/TPWRD.2009.2035426](https://doi.org/10.1109/TPWRD.2009.2035426).
- [16] D. Pylarinos, K. Theofilatos, K. Siderakis, E. Thalassinakis, I. Vitellas, A. T. Alexandridis, and E. Pyrgioti, "Investigation and classification of field leakage current waveforms," *IEEE Trans. Dielectr. Electr. Insul.*, vol. 19, no. 6, pp. 2111–2118, Dec. 2012, doi: [10.1109/TDEI.2012.6396971](https://doi.org/10.1109/TDEI.2012.6396971).
- [17] H. H. Kordkheili, H. Abravesh, M. Tabasi, M. Dakhem, and M. M. Abravesh, "Determining the probability of flashover occurrence in composite insulators by using leakage current harmonic components," *IEEE Trans. Dielectr. Electr. Insul.*, vol. 17, no. 2, pp. 502–512, Apr. 2010, doi: [10.1109/TDEI.2010.5448106](https://doi.org/10.1109/TDEI.2010.5448106).
- [18] *Selection and Dimensioning of High-Voltage Insulators Intended for Use in Polluted Conditions—Part 1: Definitions, Information and General Principles*, Standard IEC TS 60815-1:2008, International Electrotechnical Commission, 2018, pp. 1–2, [Online]. Available: <http://papers3://publication/uuid/88519C43-BEA6-4CA0-909D-FA19A25647BB>
- [19] R. Sundararajan and R. S. Gorur, "Role of non-soluble contaminants on the flashover voltage of porcelain insulators," *IEEE Trans. Dielectr. Electr. Insul.*, vol. 3, no. 1, pp. 113–118, Feb. 1996, doi: [10.1109/94.485522](https://doi.org/10.1109/94.485522).
- [20] S. C. Oliveira, E. Fontana, and F. J. do Monte de Melo Cavalcanti, "Real-time monitoring of the leakage current of 230-kV glass-type insulators during washing," *IEEE Trans. Power Del.*, vol. 24, no. 4, pp. 2257–2260, Oct. 2009, doi: [10.1109/TPWRD.2009.2016814](https://doi.org/10.1109/TPWRD.2009.2016814).
- [21] E. Fontana, J. F. Martins-Filho, S. C. Oliveira, F. J. M. M. Cavalcanti, R. A. Lima, G. O. Cavalcanti, T. L. Prata, and R. B. Lima, "Sensor network for monitoring the state of pollution of high-voltage insulators via satellite," *IEEE Trans. Power Del.*, vol. 27, no. 2, pp. 953–962, Apr. 2012, doi: [10.1109/TPWRD.2012.2183623](https://doi.org/10.1109/TPWRD.2012.2183623).
- [22] D. Pylarinos, K. Siderakis, E. Thalassinakis, E. Pyrgioti, I. Vitellas, and S. L. David, "Online applicable techniques to evaluate field leakage current waveforms," *Electr. Power Syst. Res.*, vol. 84, no. 1, pp. 65–71, Mar. 2012, doi: [10.1016/j.epsr.2011.10.009](https://doi.org/10.1016/j.epsr.2011.10.009).
- [23] M. E. Ibrahim and A. M. Abd-Elhady, "Rogowski coil transducer-based condition monitoring of high voltage insulators," *IEEE Sensors J.*, vol. 20, no. 22, pp. 13694–13703, Nov. 2020, doi: [10.1109/JSEN.2020.3005223](https://doi.org/10.1109/JSEN.2020.3005223).

- [24] T. Suda, "Frequency characteristics of leakage current waveforms of a string of suspension insulators," *IEEE Trans. Power Del.*, vol. 20, no. 1, pp. 481–487, Jan. 2005, doi: [10.1109/TPWRD.2004.837668](https://doi.org/10.1109/TPWRD.2004.837668).
- [25] A. A. Salem, R. Abd-Rahman, S. A. Al-Gailani, Z. Salam, M. S. Kamarudin, H. Zainuddin, and M. F. M. Yousof, "Risk assessment of polluted glass insulator using leakage current index under different operating conditions," *IEEE Access*, vol. 8, pp. 175827–175839, 2020, doi: [10.1109/ACCESS.2020.3026136](https://doi.org/10.1109/ACCESS.2020.3026136).
- [26] S. Chandrasekar and C. Kalaivanan, "Investigations on harmonic contents of leakage current of porcelain insulator under polluted conditions," in *Proc. 15th Nat. Power Syst. Conf. (NPSC)*, Dec. 2008, pp. 340–344.
- [27] N. Bashir and H. Ahmad, "Odd harmonics and third to fifth harmonic ratios of leakage currents as diagnostic tools to study the ageing of glass insulators," *IEEE Trans. Dielectr. Electr. Insul.*, vol. 17, no. 3, pp. 819–832, Jun. 2010, doi: [10.1109/TDEL.2010.5492255](https://doi.org/10.1109/TDEL.2010.5492255).
- [28] S. Zurek, "FEM simulation of effect of non-uniform air gap on apparent permeability of cut cores," *IEEE Trans. Magn.*, vol. 48, no. 4, pp. 1520–1523, Apr. 2012.
- [29] A. Chauhan and R. Vaish, "Magnetic material selection using multiple attribute decision making approach," *Mater. Des.*, vol. 36, pp. 1–5, Apr. 2012, doi: [10.1016/j.matdes.2011.11.021](https://doi.org/10.1016/j.matdes.2011.11.021).
- [30] L. Zhang, S. Ji, S. Gu, X. Huang, J. E. Palmer, W. Giewont, F. F. Wang, and L. M. Tolbert, "Design considerations for high-voltage insulated gate drive power supply for 10-kV SiC MOSFET applied in medium-voltage converter," *IEEE Trans. Ind. Electron.*, vol. 68, no. 7, pp. 5712–5724, Jul. 2021, doi: [10.1109/TIE.2020.3000131](https://doi.org/10.1109/TIE.2020.3000131).
- [31] *Artificial Pollution Tests on High-Voltage Insulators to be Used on A.C. Systems*, document IEC 60507, International Electrotechnical Commission, Geneva, Switzerland, 2013.



FERNANDO HUENUPÁN received the B.Sc. degree in electronic engineering from the University of La Frontera, Temuco, Chile, in 2004, and the Ph.D. degree in electrical engineering from the University of Chile, Santiago, Chile, in 2010. He has been an Associate Professor with the Electrical Engineering Department, University of La Frontera, since 2010. His research interests include pattern recognition, multiple classifier systems, and robustness in speech technology.



FRANCISCO VALLEJOS was born in Santiago, Chile, in 1992. He received the Engineering degree in electrical engineering from the Universidad de la Frontera, Temuco, in 2016.



RODRIGO J. VILLALOBOS received the Engineering degree in electrical engineering from the University of Concepción, Concepción, Chile, in 2006, and the master's (Professional) degree in electrical engineering from Université Paris-Sud, Orsay, France, in 2008. He is currently pursuing the Ph.D. degree with the University of Concepción. From 2008 to 2015, he was a Project Manager of the Power Transmission Industry in Chile, developing projects of power substations and transmission lines, until 220 kV. Since 2015, he has been with the Electrical Engineering Department, University of La Frontera, Temuco. His research interests include power transmission systems, insulation in power systems, and practical solutions equipment for the challenge of power transmission systems industry. In 2017 and 2021, he received an important research fund (FONDEF) with the National Commission for Scientific and Technological Research (ANID) of Chile for the development of an equipment for monitoring of pollution level on insulators.



LUIS A. MORAN (Fellow, IEEE) was born in Concepción, Chile. He received the degree in electrical engineering from the University of Concepción, Concepción, in 1982, and the Ph.D. degree from Concordia University, Montreal, PQ, Canada, in 1990. Since 1990, he has been with the Electrical Engineering Department, University of Concepción, where he is a Professor. He has written and published more than 60 transaction papers in the design of static converters for power system dynamic compensation (Var Compensators and Active Power Filters) and power quality issues in industrial power distribution systems. He has more than 30 year's of full-time teaching and research activities, including short courses for industry and utility companies and concurrent experience as industrial consultant. He has extensive consulting experience in mining industry, especially in the application of medium voltage AC drives, large power cycloconverter drives for grinding mills, power quality issues, power system protections, and active power system compensation. His research interests include medium voltage AC drives, power quality, active power filters, flexible AC transmission systems, and power protection systems.



ROBERTO MONCADA was born in Chillan, Chile. He received the degree in electrical engineering and the Doctor degree in electrical engineering from the University of Concepcion, Concepción, Chile, in 2006 and 2012, respectively. Currently, he is with the Universidad de La Frontera, Temuco, Chile, as an Associate Professor, in the area of electrical machines. His research interests include permanent-magnet machines design and control, synchronous reluctance machines, power electronics, renewable energy, and energy efficiency.



CRISTIAN PESCE G. (Member, IEEE) received the degree in electronic engineering from the Pontificia Universidad Católica de Valparaíso, Valparaíso, Chile, in 2003, the M.Sc. degree in electrical engineering from the University of La Frontera, Temuco, Chile, in 2010, and the D.Sc. degree in electrical engineering from the University of Concepción, Concepción, Chile, in 2017. He is currently an Assistant Professor with the Department of Electrical Engineering, University of La Frontera, Temuco, Chile. His research interests include design and control of power converters applied to electric power systems and electrical machines and drives.

...